International Journal of Innovative Research and Scientific Studies, 8(5) 2025, pages: 1137-1146

IJIRSS
International Journal of Innovative Research & Scientific Studies

ISSN: 2617-6548

URL: www.ijirss.com

Brain cyst detection using deep learning models

Aziz Ilyas Ozturk[1*], Osman Yildirim[2], Kamil Kaygusuz[3], Ebru Idman[4], Emrah Idman[5]

[1]*General Electric Healthcare, Istanbul, Turkey.*
[2,5]*Istanbul Aydin University, Faculty of Engineering, Department of Electrical and Electronics Engineering, Istanbul, Turkey.*
[3]*Istanbul Aydin University, Faculty of Engineering, Department of Mechanical Engineering, Istanbul, Turkey.*
[4]*Istanbul Arel University, Vocational School, Department of Computer Technologies, Istanbul, Turkey.*

Corresponding author: Aziz Ilyas Ozturk (*Email: aziz.ozturk@gehealthcare.com*)

Abstract

Cysts are common in healthcare and can be associated with various diseases. They can develop in different body parts and contain fluid, semi-solid, or air. Brain cysts are masses that form in the brain, and surgical methods may be used to treat them. The importance of deep learning in medical imaging is steadily growing. This study attempted to detect brain cysts using various architectures, including Random Forest, Unet, AlexNet, and LeNet. The Random Forest algorithm was found to be more successful than the other algorithms. This algorithm is crucial for classification and regression problems as it trains a series of decision trees and consolidates their predictions to create a robust and powerful model. Magnetic resonance imaging was used to detect cysts. The accuracy rates for cyst detection were 79.52%, 89.99%, 90.41%, and 97.26%, respectively. Several models were employed for this purpose, including LeNet, AlexNet, Unet, and the Random Forest algorithm. The accuracy rates for cyst detection were 79.52%, 89.99%, 90.41%, and 97.26%, respectively.

Keywords: Brain cyst, Deep learning, Random forest algorithm.

DOI: 10.53894/ijirss.v8i5.8974
Funding: This study received no specific financial support.
History: Received: 20 June 2025 / **Revised:** 24 July 2025 / **Accepted:** 28 July 2025 / **Published:** 31 July 2025

Competing Interests: The authors declare that they have no competing interests.
Authors' Contributions: All authors contributed equally to the conception and design of the study. All authors have read and agreed to the published version of the manuscript.
Transparency: The authors confirm that the manuscript is an honest, accurate, and transparent account of the study; that no vital features of the study have been omitted; and that any discrepancies from the study as planned have been explained. This study followed all ethical practices during writing.
Institutional Review Board Statement: This study was conducted using MRI data obtained from the Istanbul Betatom Imaging Center. All personally identifiable information was removed from the images prior to analysis. The use of these anonymized data was approved by the Istanbul Betatom Imaging Center, and the approval email is available upon request. All procedures were carried out in accordance with institutional ethical guidelines.
Publisher: Innovative Research Publishing

1. Introduction

Cysts may contain air and liquid and can form in various body tissues. They can range in size from small to potentially harmful over time as they grow and affect surrounding tissues.

These fluid-filled sacs are often benign, but their presence in critical areas such as the brain can lead to significant clinical concerns. Depending on their location and growth rate, cysts may exert pressure on adjacent tissues, potentially disrupting normal physiological functions. In the brain, even small cysts can interfere with neural pathways, leading to symptoms ranging from mild discomfort to severe neurological deficits. Early detection and accurate classification of these cysts are essential for timely intervention and effective treatment planning. With the advancement of imaging technologies and computational methods, non-invasive diagnostic tools have become increasingly important in clinical decision-making.

Arachnoid cysts, a type of brain cyst, are benign and occasionally observed. They can be asymptomatic or present with neuropsychiatric symptoms [1, 2]. Arachnoid cysts have been the subject of case studies, focusing on their effects on bipolar and psychotic disorders rather than obsessive-compulsive disorder [2, 3].

The most common symptom associated with arachnoid cysts is a headache, which is often caused by localized pressure. Cognitive impairment may also be present [4, 5]. Arachnoid cysts, which account for 1% of intracranial lesions, are typically located in the middle cranial fossa, with a higher prevalence on the left side than on the right [6-8]. The existing literature has primarily focused on arachnoid cysts and their potential psychiatric implications, with publications mainly consisting of case reports [9, 10].

Several studies in the literature have employed machine learning to investigate brain tumors. This study examines the diagnosis of brain cysts and its contribution to the fields of medical imaging and machine learning. The Brainmrnet architecture was compared with AlexNet, LeNet, and VGG16 architectures and achieved a success rate of 96.05% [11]. The Unet architecture was used and reached a level of 86% in a related study [12]. An accuracy of 92% was achieved with the Random Forest architecture [13] while Kernel SVM reached 90.4% accuracy [14]. A MobileNetV2 model was used to achieve a 95.27% result in a study on skin cancer detection[15].

In this study on brain cysts, the authors compared the results obtained with AlexNet, LeNet, U-Net, and Random Forest algorithms after enhancing the images in each algorithm. The results were 79.2% with LeNet, 89.99% with AlexNet, 90.41% with U-Net, and 97.26% with the Random Forest algorithm.

2. Literature Review

Recent advancements in artificial intelligence (AI) have significantly impacted the field of medical imaging, particularly in the automated detection of brain anomalies. Deep learning (DL) techniques, especially convolutional neural networks (CNNs), have proven effective in various medical classification and segmentation tasks [16]. These models can automatically learn spatial hierarchies of features from input images, reducing the need for manual feature extraction.

In the field of brain pathology detection, CNN-based architectures such as VGGNet, ResNet, and DenseNet have been used to classify tumors, cysts, and other abnormalities with high accuracy [17]. A deep CNN approach for brain tumor segmentation using multi-modal MRI data has shown competitive results on the BRATS dataset [18]. Similarly, the use of a fine-tuned VGG16 model has demonstrated effectiveness in identifying glioma and meningioma tumors from T1-weighted MRI images [19].

Beyond deep learning, classical machine learning models such as Support Vector Machines (SVM), k-Nearest Neighbors (k-NN), and Random Forest (RF) continue to offer strong performance, particularly when paired with well-crafted feature extraction techniques [20]. RF, in particular, has been recognized for its robustness, ability to handle high-dimensional data, and resistance to overfitting, especially in settings with limited annotated data [21].

Hybrid approaches that combine DL-based feature extraction with traditional classifiers have also gained traction. For instance, combining Capsule Networks with Random Forest classifiers has proven that ensemble models can outperform end-to-end CNNs on small datasets [22]. Similarly, using pre-trained CNNs to extract features from MRI images and applying Random Forest for classification has yielded high diagnostic performance in Alzheimer's detection [23].

Additionally, transfer learning has become an effective strategy in medical imaging due to the scarcity of labeled data. Pre-trained models on natural image datasets (e.g., ImageNet) can be fine-tuned for medical tasks, significantly reducing training time and improving accuracy [24]. These approaches are particularly effective when combined with domain-specific preprocessing techniques, such as histogram equalization or bilateral filtering.

In summary, the literature suggests that both deep learning and classical machine learning approaches have distinct strengths in medical imaging. The integration of robust preprocessing techniques and hybrid learning models remains a promising direction, especially for brain cyst detection tasks involving limited data and class imbalance.

3. Materials and Methods

As material, MRI data without personal information from patients were obtained from the Istanbul Betatom Imaging Center. There were a total of 2,194 brain images, including cystic and non-cystic cases. The images are 512x512 pixels in JPG format, with a size of 146 KB each. Twenty percent of the data was used for testing and eighty percent for training. The images were enhanced and applied to pre-trained algorithms. An example of a cystic and non-cystic image from the dataset is shown in Figure 1, with the cystic image on the left and the non-cystic image on the right.

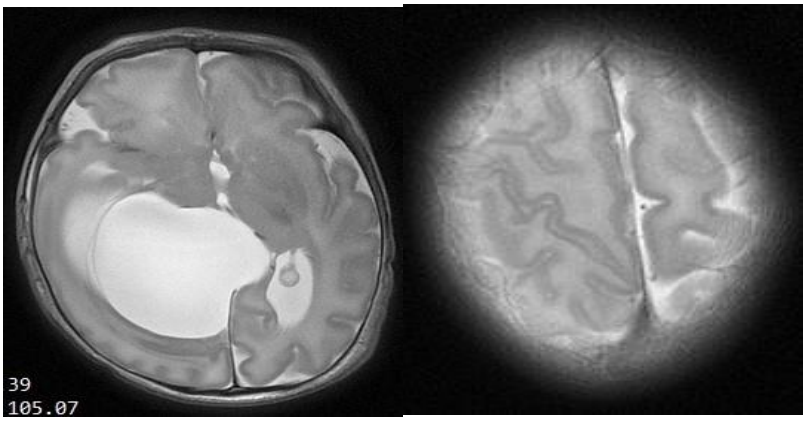

Figure 1.
Cystic and Non-cystic Sample Images.

3.1. Image Enhancement

In this study, the Bilateral Filter and the Laplacian Sharpening Filter were used to enhance the image.

These enhancement techniques improve the visibility of structural details in MRI scans, which is crucial for accurate feature extraction. By reducing noise and emphasizing edges, the filters help the models focus on relevant anatomical patterns. This preprocessing step significantly contributes to the overall performance of the classification algorithms.

3.2. Bilateral Filter

The bilateral filter is a commonly used image processing technique that preserves edges while reducing noise. It achieves this by comparing each pixel with other pixels within a certain filter size and weighting the values of color and spatial similarity according to their respective standard deviations (sigmacolor and sigmaspace). The resulting filter is then applied to the pixels within the filter size, resulting in a new assigned value.

This method is particularly effective in medical imaging, where preserving fine anatomical structures is essential. By maintaining edge integrity while smoothing homogeneous regions, the bilateral filter enhances the clarity of critical features such as cyst boundaries. This balance between noise reduction and detail preservation makes it a valuable preprocessing step for improving model accuracy.

3.3. Laplacian Sharpening Filter

The purpose of this application is to highlight edges and contrast in an image. It achieves this by identifying differences or changes in the image, which in turn highlights edges. The Laplacian filter is used to calculate the second derivative of pixel values in an image. The steps involved in Laplacian sharpening are as follows: convolution is applied to the image using the Laplacian filter, each pixel is multiplied by and summed with its surrounding pixels, and the resulting filtered image is added to the original image to sharpen it.

This sharpening technique is especially useful in highlighting subtle structural differences in medical images. Enhancing the contrast between adjacent regions allows for clearer visualization of cyst boundaries and other anomalies. This improved clarity supports more accurate feature extraction and contributes to the overall effectiveness of the classification models used in the study.

3.4. Lenet

LeNet is widely recognized as one of the pioneers of Convolutional Neural Network (CNN) architectures. It was originally developed in Lecun et al. [25]. The network extracts features from input data using convolutional layers. The feature maps obtained from these layers are then used to reduce their size and emphasize important information, which can enhance the model's generalization ability. LeNet employs activation functions such as sigmoid and tanh to learn more complex relationships.

Lenet works with small black-and-white images, typically with dimensions of 32x32 pixels. The language is clear, objective, and value-neutral, with consistent technical terms and common sentence structure. The first convolutional layer creates six 5x5 filters to apply convolutional operations on the input image. A maximum pooling layer follows to reduce the convolution results and emphasize the features. The text is free from grammatical errors, spelling mistakes, and punctuation errors. The text adheres to style guides, uses consistent citations, and follows a consistent footnote style and formatting features. The language is formal, avoiding contractions, colloquial words, informal expressions, and unnecessary jargon. The text is structured with a logical progression and causal connections between statements. The content of the improved text is as close as possible to the source text, and no further aspects have been added. The second convolutional layer has 16 filters of size 5x5 and is followed by another maximum pooling layer. The fully connected layers in this model consist of a flattening layer that converts the outputs of the convolution and pooling layers into a one-dimensional vector. This is followed by a fully connected layer with 120 neurons that processes the outputs using the ReLU activation function. Another fully connected layer with 84 neurons follows, also processed with ReLU. The output layer is responsible for classification and uses the softmax activation function to calculate the probability distribution among the classes [26, 27].

3.5. AlexNet

AlexNet is a deep learning model that won the ImageNet Large Scale Visual Recognition Challenge in 2012. It was trained on a large dataset and achieved significant success in image recognition. The model consists of five convolutional layers that identify and learn features of images through convolution operations. The pooling layers summarize the convolution results by reducing dimensions and employing maximum pooling operations. The ReLU activation function is used in all hidden layers of AlexNet. AlexNet has three fully connected layers that utilize features extracted from the convolutional and pooling layers for final classification. To enhance the model's generalization ability and reduce overfitting, regularization is applied by randomly dropping specific neurons.

AlexNet operates with 224x224 pixel RGB images and has five convolutional layers that generate feature maps. The initial convolutional layer has an 11x11 filter, while the subsequent layers use 3x3 or 5x5 filters. All layers apply the ReLU activation function after the first convolutional layer. To reduce the size of the feature maps, three max pooling layers are included. In order to improve the model's generalization ability, a normalization layer is added between the convolutional layers. For classification, three fully connected layers are used, taking into account the results from previous convolutional and pooling layers. After the first two layers, the ReLU function is applied. The last layer, which has a number of neurons equal to the class count, uses softmax for classification. Dropout is implemented to prevent overfitting by randomly deactivating neurons during training [28, 29].

3.6. Unet

UNet is a deep learning algorithm specifically designed for biomedical image segmentation. It was introduced by Ronneberger and colleagues in 2015. The algorithm has a symmetric structure with transposed convolution layers located after many convolution layers. The feature maps obtained in convolution layers have similar scales and are added in transpose layers, allowing the network to merge features at different sizes. The UNet network has different depths between the input and output layers, which allows for the learning of features at various levels. The output layer of UNet represents a channel for each class per pixel, with sigmoid typically used in this layer to express the probability of belonging for each pixel.

This architecture is particularly effective in medical imaging tasks, as it enables precise localization of features. Its design ensures that both the global context and fine details are preserved.

The encoder section of Unet includes convolution layers to extract features, each of which includes ReLU and mostly double-strided convolution operations. Increasing the number of layers results in a more abstract and broad representation of feature maps. Skip connections are created by adding feature maps obtained at each encoder layer to the corresponding decoder layer of the same depth. These skip connections allow the network to enhance higher-level features using lower-level features, resulting in better localization. The data from the encoder is transmitted to the decoder through skip connections. The decoder section comprises transposed convolution layers that learn and generate features across a wide range. ReLU is utilized in these layers. The output layer employs the sigmoid function, which includes a channel for each class per pixel [30-33].

3.7. Random Forest Algorithm

The Random Forest algorithm is a machine learning algorithm that can be used for both classification and regression problems. It is formed by the combination of many decision trees, which are trained with random features.

Each decision tree in the forest contributes a vote to the final prediction, which enhances the model’s robustness and reduces the risk of overfitting. This ensemble approach ensures that the model captures diverse patterns in the data. In medical imaging tasks like brain cyst detection, this diversity allows the algorithm to generalize better across different cases, improving diagnostic accuracy and reliability.

This algorithm is known to perform well on large and complex datasets. During the training of each decision tree, random subsamples are taken from the dataset, which include features and target variables. Random subsets of features are selected when training decision trees, allowing each tree to be trained on different samples and ensuring their independence. This subsampling and feature selection enable the training of each decision tree. By combining many decision trees to form an ensemble, the Random Forest algorithm creates a classification based on the majority of trees in the ensemble. The ensemble forms a more robust and generalizable model. When making predictions on new examples, it combines the predictions of each tree to generate an overall prediction [34-37].

4. Discussion

Brain cysts can cause a range of symptoms, including headaches, visual and auditory impairments, cognitive disorders, and abnormal head growth, depending on their type and size. This study compares the performance of LeNet, AlexNet, U-Net, and Random Forest algorithms in detecting brain cysts. The study was conducted in the Python environment, and after applying image enhancement to the loaded data for LeNet, the training and validation losses during the training iterations and accuracy changes are shown in Figure 2.

The LeNet algorithm achieved an accuracy of 79.52%.

The relatively lower performance of LeNet can be attributed to its architectural limitations. Designed for small-scale grayscale images, LeNet lacks the depth and complexity necessary to capture high-level spatial features in MRI images of the brain. Additionally, its reliance on fewer convolutional layers and older activation functions such as tanh and sigmoid may restrict its ability to generalize well in a medical imaging context, especially in high-resolution data environments.

These findings align with previous literature, where LeNet demonstrated suboptimal performance in complex biomedical classification tasks.

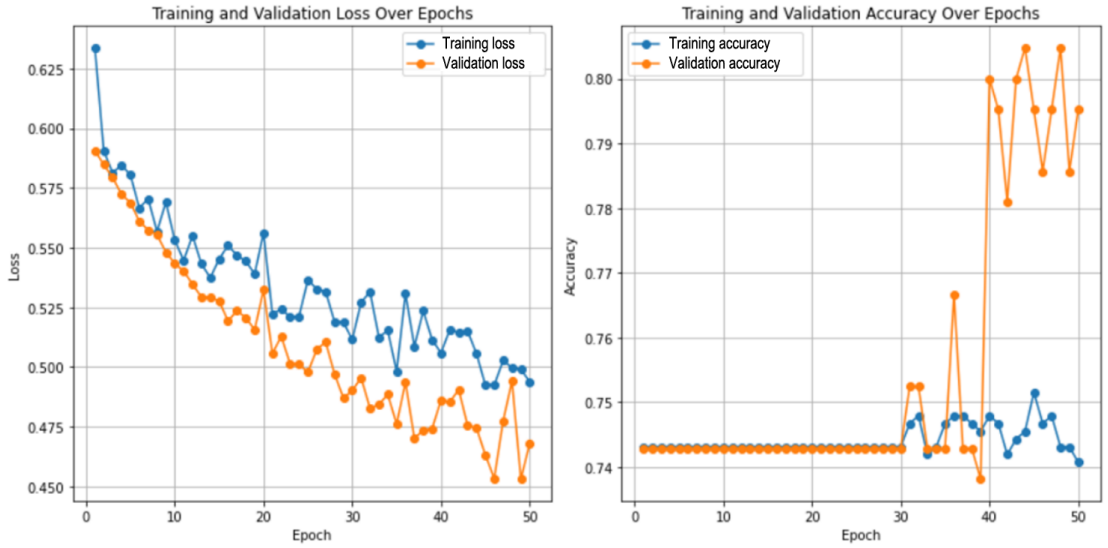

Figure 2.
Change Graph of Training and Validation Losses Across Training Iterations and Accuracy

Figure 3 shows the change graph of training and validation losses across training iterations and accuracy in the study conducted using the Python environment for AlexNet.

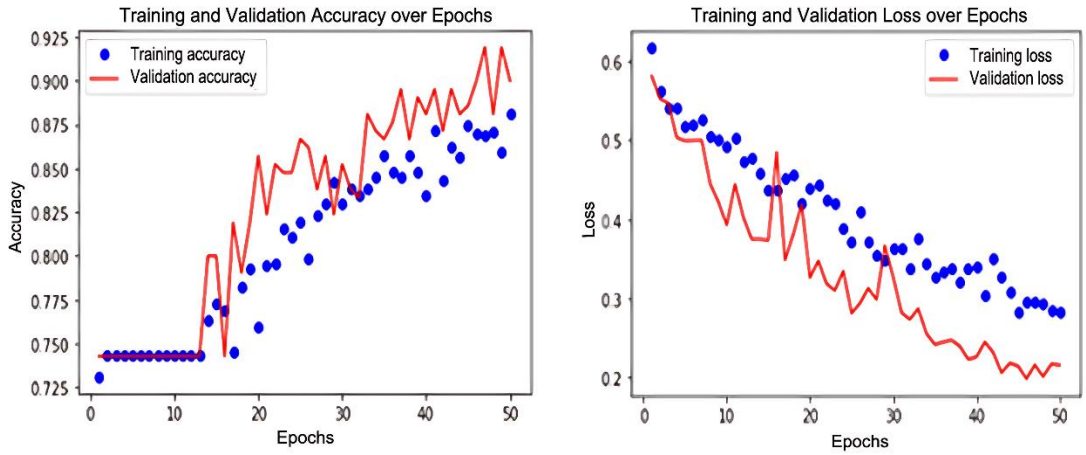

Figure 3.
Change Graph of Training and Validation Losses Across Training Iterations and Accuracy.

AlexNet achieved an accuracy of 89.99%. The study's findings for Unet are presented in Figure 4.

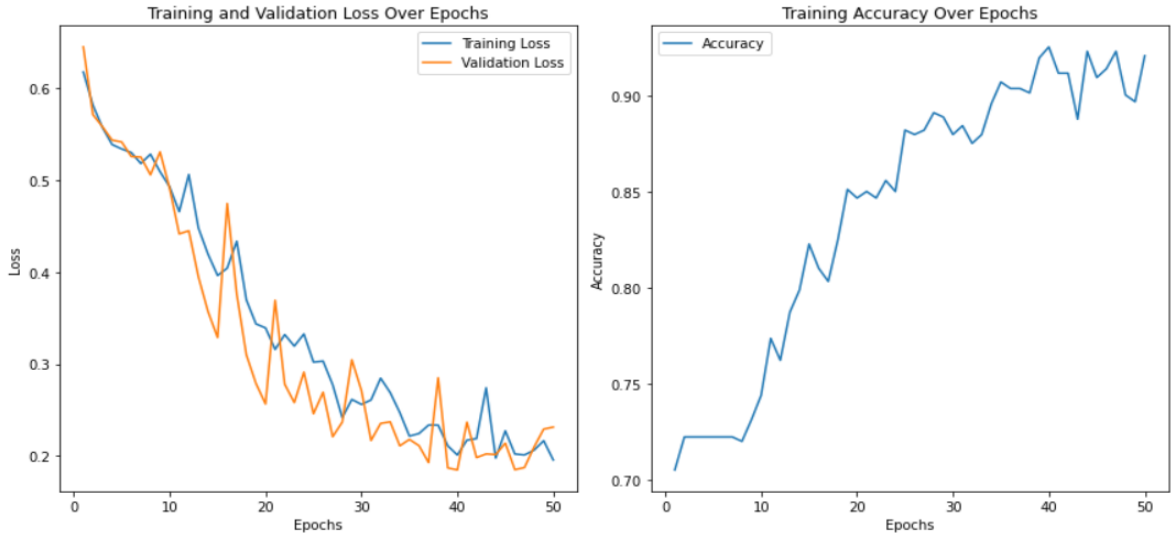

Figure 4.
Unet Output Graphs.

The Unet outputs achieved an accuracy result of 90.41%. Figures 5 and 6 show the outputs for another algorithm, the Random Forest Algorithm.

The improved performance of AlexNet and Unet over LeNet suggests that deeper architectures with more advanced convolutional hierarchies are better suited for extracting relevant features in brain MRI images. Unet, in particular, offers an advantage with its encoder-decoder structure and skip connections, allowing both low-level texture and high-level semantic information to be retained. This makes Unet a strong candidate for medical image segmentation tasks where lesion localization is important. However, in this study, Unet was used for classification, not segmentation, which might explain why its performance, while high, did not surpass that of the Random Forest model.

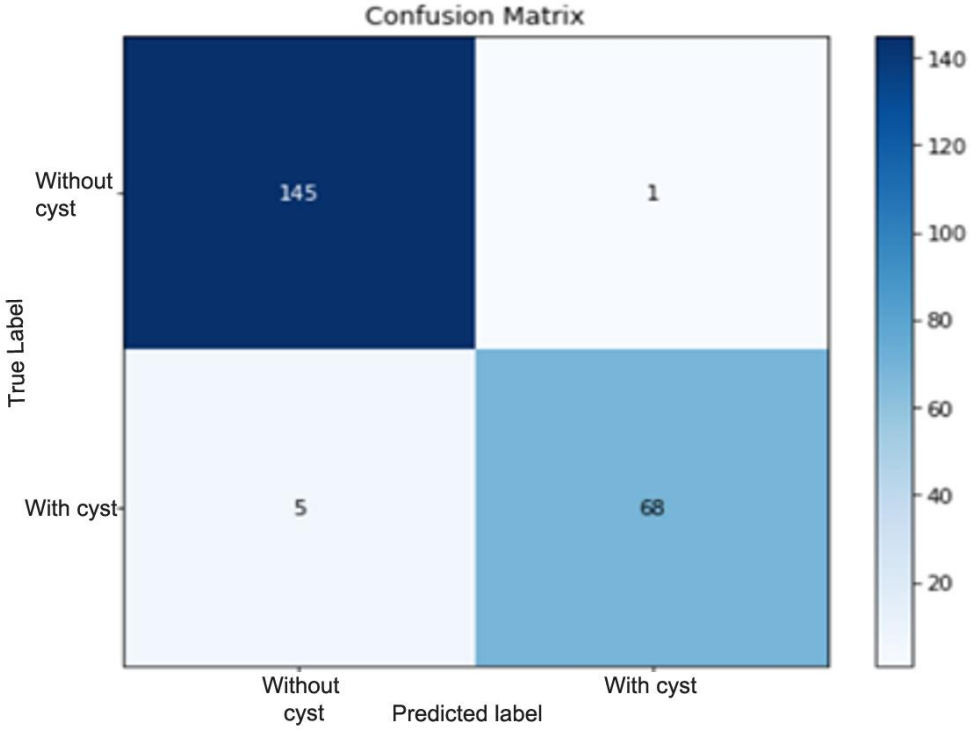

Figure 5.
Confusion Matrix.

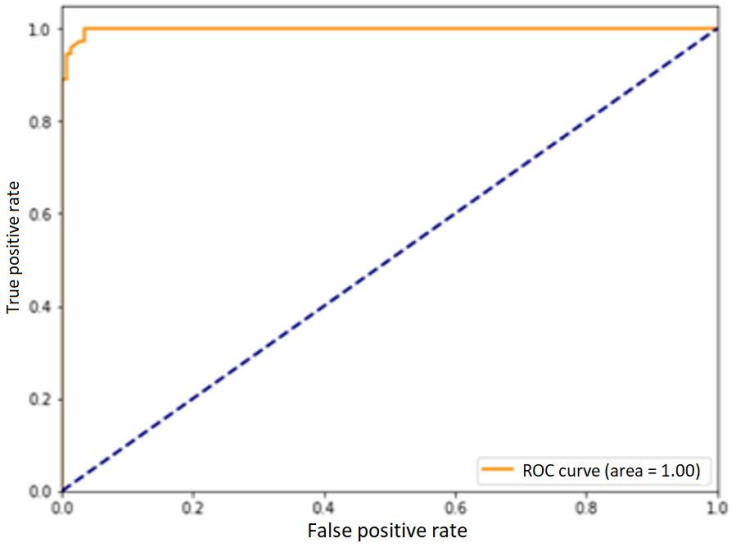

Figure 6.
Receiver Operating Characteristic Curve.

The Confusion Matrix is a tool used to evaluate the performance of algorithms in classification modeling. True Positive (TP) indicates when the model correctly predicts a positive example, such as correctly diagnosing a disease as positive. True Negative (TN) represents when the algorithm correctly predicts negative, indicating a correct negative diagnosis, i.e., the person is healthy. False positives (FP) and False negatives (FN) are two types of errors that can occur in classification models. FP occurs when the model incorrectly identifies a positive instance as negative, while FN occurs when the model incorrectly identifies a negative instance as positive. FP occurs when the model incorrectly identifies a positive instance as negative, while FN occurs when the model incorrectly identifies a negative instance as positive.

The Receiver Operating Characteristic (ROC) is a graphical representation used to evaluate the performance of classification models. The ROC curve illustrates the relationship between sensitivity and specificity. Sensitivity is the true positive rate, calculated by dividing true positives by the total number of positive examples. Specificity is the true negative rate, calculated by dividing true negatives by the total number of negative examples. The axes range from 0 to 1, with high sensitivity and high specificity represented by values closer to 1. It is important to note that the closer the ROC curve is to the top-left corner, the better the model performs. The model's performance can be quantified by measuring the area under the ROC curve, which ranges from 0 to 1. The closer the value is to 1, the better the algorithm's performance.

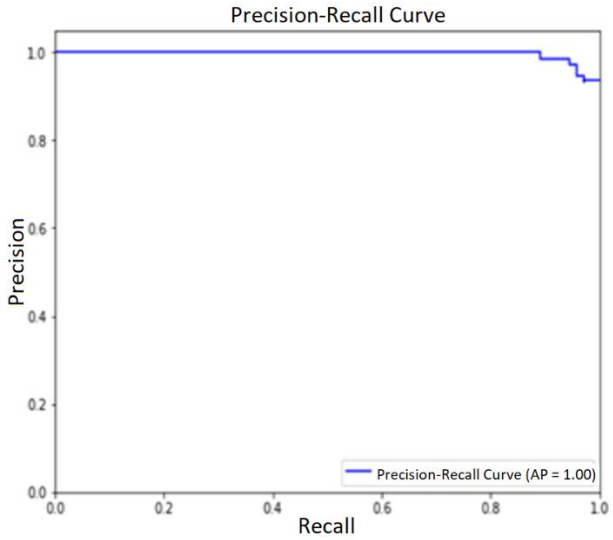

Figure 7.
Precision-Recall Curve.

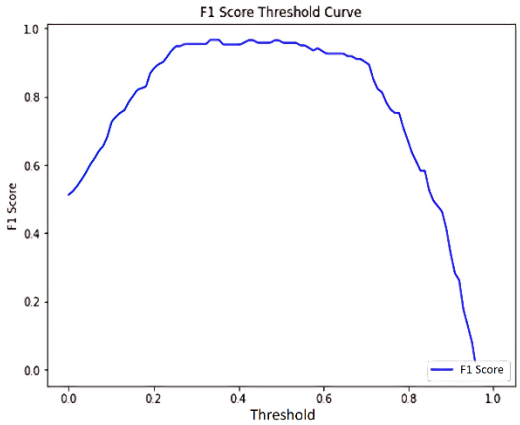

Figure 8.
F1 Score – Threshold Curve.

In cases of imbalanced classifications, the Precision-Recall curve may be preferred over the ROC curve. A model with an average precision (AP) value of 1 indicates good performance, with high precision and recall values at every possible threshold, suggesting effective detection of positive classifications and a low probability of false positives.

The F1 score and Threshold Curve graph exhibit a Gaussian curve characteristic. The curve's peak indicates the threshold value at which the model performs best. A symmetrical shape, such as the Gaussian curve, suggests that the model performs similarly well at various threshold values.

The Random Forest Algorithm was used, resulting in the best performance with an accuracy rate of 97.26%.

The superior accuracy of the Random Forest algorithm, despite it being a classical machine learning model, highlights the importance of feature selection and ensemble learning in small-to-medium medical imaging datasets. Random Forest's inherent ability to handle high-dimensional data and its robustness to overfitting due to bootstrap aggregation make it particularly effective in binary classification tasks such as cyst detection. Moreover, its interpretability and lower computational cost compared to deep neural networks make it a practical tool in clinical settings where computational resources and annotated data are limited. In our study, the Random Forest-based model demonstrated superior classification accuracy, highlighting the effectiveness of ensemble learning methods when combined with optimized preprocessing techniques. This discrepancy might stem from the enhanced image preprocessing steps applied in our study or the relatively balanced class distribution. While many studies focus solely on deep learning approaches, our inclusion of Random Forest offers a compelling alternative, particularly for centers with limited computational infrastructure. These findings contribute to the growing evidence that classical models, when combined with optimized data preprocessing, can achieve or even surpass deep learning in certain diagnostic imaging tasks.

Furthermore, the success of the Random Forest model in this context underscores the value of model simplicity and interpretability in clinical applications. While deep learning models often require extensive computational resources and large annotated datasets, classical models like Random Forest can deliver competitive results with fewer resources. This makes them especially suitable for deployment in smaller healthcare facilities or research environments where infrastructure and data availability are limited.

5. Conclusion

In this study, we conducted a comprehensive comparative evaluation of multiple machine learning and deep learning models, LeNet, AlexNet, U-Net, and Random Forest, for the detection of brain cysts using enhanced magnetic resonance imaging (MRI) data. The integration of image enhancement techniques, specifically Bilateral Filtering and Laplacian Sharpening, facilitated improved feature extraction, contributing to the accuracy of the models evaluated.

The Random Forest algorithm outperformed the other models, achieving the highest classification accuracy at 97.26%, followed by Unet (90.41%), AlexNet (89.99%), and Lenet (79.52%). The superior performance of Random Forest highlights the continued relevance of ensemble-based classical machine learning algorithms, especially when dealing with moderate-sized, high-dimensional, and possibly imbalanced datasets where deep learning models may not always generalize optimally due to limited data availability.

One of the key strengths of this study is the methodological diversity it introduces into the brain cyst detection domain by not restricting the evaluation solely to deep learning approaches but including traditional ensemble methods. This broader approach allows for a more nuanced understanding of algorithmic performance in practical clinical scenarios, where data quality, quantity, and heterogeneity often present significant challenges. Furthermore, the utilization of multiple evaluation metrics, including accuracy, precision-recall curves, F1 scores, and ROC analysis, provided a multidimensional assessment of model performance, offering a more robust and clinically relevant evaluation than accuracy alone.

However, this study has certain limitations that warrant consideration. Firstly, the dataset was derived from a single imaging center and consisted of 2,194 images, which, while useful for initial evaluation, may not fully capture the diversity and variability present in larger, multi-center, and multi-vendor datasets. The relatively limited sample size and the absence of external validation cohorts may affect the generalizability of the findings. Secondly, the current work primarily focused on binary classification (cystic vs. non-cystic) without incorporating cyst subtypes or evaluating the impact of cyst size,

location, and morphology, all of which may carry significant clinical relevance. Furthermore, while image enhancement techniques were applied, the study did not explore advanced data augmentation strategies or domain adaptation methods that could potentially increase model robustness and generalizability.

The findings of this study hold important implications for future research in automated medical image analysis, particularly in scenarios where limited annotated data are available. The demonstrated success of Random Forest suggests that hybrid approaches integrating classical machine learning with deep learning-based feature extraction may offer a promising direction for future studies. Combining the hierarchical feature learning capabilities of deep neural networks with the robust generalization properties of ensemble methods like Random Forest could potentially yield even higher performance, especially in complex, heterogeneous datasets.

Future work should also focus on expanding the dataset to include images from multiple institutions, vendors, and patient populations to assess model scalability and generalizability. Incorporating multimodal data, such as clinical parameters, patient history, and other imaging modalities, could further enhance model performance and clinical applicability. Additionally, implementing explainable AI (XAI) frameworks would improve model interpretability, facilitating clinician trust and eventual integration into clinical workflows.

In conclusion, while deep learning remains at the forefront of medical image analysis research, this study underscores the continued relevance of ensemble methods such as Random Forest in specific clinical imaging contexts. The insights provided here contribute to the ongoing discourse on optimal model selection for brain cyst detection and may serve as a reference framework for future investigations aiming to bridge the gap between algorithmic development and clinical deployment.

References

[1] G. Baquero, P. Molero, J. Pla, and F. Ortuño, "A schizophrenia-like psychotic disorder secondary to an arachnoid cyst remitted with neurosurgical treatment of the cyst," *The Open Neuroimaging Journal*, vol. 8, p. 1, 2014.

[2] J. A. Da Silva, A. Alves, M. Talina, S. Carreiro, J. Guimarães, and M. Xavier, "Arachnoid cyst in a patient with psychosis: Case report," *Annals of General Psychiatry*, vol. 6, no. 1, p. 16, 2007.

[3] A. Hegde, A. Ghosh, S. Grover, A. Kumar, and R. Chabbra, "Arachnoid cyst masquerades as late onset obsessive–compulsive disorder," *General Hospital Psychiatry*, vol. 36, no. 1, p. 125, 2014.

[4] C. A. Helland and K. Wester, "A population-based study of intracranial arachnoid cysts: Clinical and neuroimaging outcomes following surgical cyst decompression in children," *Journal of Neurosurgery: Pediatrics*, vol. 105, no. 5, pp. 385-390, 2006.

[5] C. J. Shin, M. Rho, Y. S. Won, and S. O. Kim, "Rapid visual deterioration caused by posterior fossa arachnoid cyst," *Journal of Korean Neurosurgical Society*, vol. 59, no. 3, pp. 314-318, 2016.

[6] B. Bakim *et al.*, "Arachnoid cyst and bipolar disorder: A case report," *Psychiatry and Behavioral Sciences*, vol. 2, no. 2, p. 70, 2012.

[7] J. A. Gosalakkal, "Intracranial arachnoid cysts in children: A review of pathogenesis, clinical features, and management," *Pediatric Neurology*, vol. 26, no. 2, pp. 93-98, 2002.

[8] K. Wester, "Gender distribution and sidedness of middle fossa arachnoid cysts: A review of cases diagnosed with computed imaging," *Neurosurgery*, vol. 31, no. 5, pp. 940-944, 1992.

[9] W. M. Bahk, C. U. Pae, J. H. Chae, T. Y. Jun, and K. S. Kim, "A case of brief psychosis associated with an arachnoid cyst," *Psychiatry and Clinical Neurosciences*, vol. 56, no. 2, pp. 203-205, 2002.

[10] B. Özdemir and M. Gülsün, "Psychotic disorder and arachnoid cyst: A case report," *Düşünen Adam,* vol. 19, pp. 217-220, 2006.

[11] M. Toğaçar, B. Ergen, and Z. Cömert, "BrainMRNet: Brain tumor detection using magnetic resonance images with a novel convolutional neural network model," *Medical Hypotheses*, vol. 134, p. 109531, 2020. https://doi.org/10.1016/j.mehy.2019.109531

[12] Ö. Çiçek, A. Abdulkadir, S. S. Lienkamp, T. Brox, and O. Ronneberger, "3D U-Net: learning dense volumetric segmentation from sparse annotation," in *International Conference on Medical Image Computing and Computer-Assisted Intervention*, 2016: Springer, pp. 424-432.

[13] V. F. Rodriguez-Galiano, B. Ghimire, J. Rogan, M. Chica-Olmo, and J. P. Rigol-Sanchez, "An assessment of the effectiveness of a random forest classifier for land-cover classification," *ISPRS Journal of Photogrammetry and Remote Sensing*, vol. 67, pp. 93-104, 2012. https://doi.org/10.1016/j.isprsjprs.2011.11.002

[14] M. Li, X. Lu, X. Wang, S. Lu, and N. Zhong, "Biomedical classification application and parameters optimization of mixed kernel SVM based on the information entropy particle swarm optimization," *Computer Assisted Surgery*, vol. 21, no. sup1, pp. 132-141, 2016.

[15] M. Toğaçar, Z. Cömert, and B. Ergen, "Intelligent skin cancer detection applying autoencoder, MobileNetV2 and spiking neural networks," *Chaos, Solitons & Fractals*, vol. 144, p. 110714, 2021.

[16] G. Litjens *et al.*, "A survey on deep learning in medical image analysis," *Medical Image Analysis*, vol. 42, pp. 60-88, 2017. https://doi.org/10.1016/j.media.2017.07.005

[17] S. Minaee, Y. Boykov, F. Porikli, A. Plaza, N. Kehtarnavaz, and D. Terzopoulos, "Image segmentation using deep learning: A survey," *IEEE Transactions on Pattern Analysis and Machine Intelligence*, vol. 44, no. 7, pp. 3523-3542, 2021.

[18] S. Pereira, A. Pinto, V. Alves, and C. A. Silva, "Brain tumor segmentation using convolutional neural networks in MRI images," *IEEE Transactions on Medical Imaging*, vol. 35, no. 5, pp. 1240-1251, 2016. https://doi.org/10.1109/TMI.2016.2538465

[19] M. S. Hossain et al, "Brain tumor detection using pre-trained VGG-16 and transfer learning," in *Proceedings of the IEEE International Conference on Computer Systems and Engineering, 57–61*, 2021.

[20] G. James, D. Witten, T. Hastie, and R. Tibshirani, *An introduction to statistical learning*, 2nd ed. New York: Springer, 2021.

[21] L. Rokach, "Ensemble-based classifiers," *Artificial Intelligence Review*, vol. 33, no. 1, pp. 1-39, 2010.

[22] P. Afshar, A. Mohammadi, and K. N. Plataniotis, "Brain tumor type classification via capsule networks," in *Proceedings of the IEEE International Conference on Image Processing (pp. 3129–3133)*, 2018.
[23] D. Zhang, Y. Wang, L. Zhou, H. Yuan, D. Shen, and A. s. D. N. Initiative, "Multimodal classification of Alzheimer's disease and mild cognitive impairment," *Neuroimage*, vol. 55, no. 3, pp. 856-867, 2011.
[24] T.-Y. Lin, P. Goyal, R. Girshick, K. He, and P. Dollár, "Focal loss for dense object detection," in *Proceedings of the IEEE International Conference on Computer Vision (pp. 2980–2988)*, 2017.
[25] Y. Lecun, L. Bottou, Y. Bengio, and P. Haffner, "Gradient-based learning applied to document recognition," *Proceedings of the IEEE*, vol. 86, no. 11, pp. 2278-2324, 1998. https://doi.org/10.1109/5.726791
[26] A. Ng, "Max pooling in convolutional neural networks," *Journal of Machine Learning Research*, vol. 19, no. 72, pp. 1–15, 2018.
[27] K. He, X. Zhang, S. Ren, and J. Sun, "Spatial pyramid pooling in deep convolutional networks for visual recognition," *IEEE Transactions on Pattern Analysis and Machine Intelligence*, vol. 37, no. 9, pp. 1904-1916, 2015.
[28] K. Simonyan and A. Zisserman, "Very deep convolutional networks for large-scale image recognition," *arXiv preprint arXiv:1409.1556*, 2014.
[29] A. Krizhevsky, I. Sutskever, and G. E. Hinton, "Imagenet classification with deep convolutional neural networks," *Advances in Neural Information Processing Systems*, vol. 25, pp. 1097–1105, 2012.
[30] L.-C. Chen et al, "Deeplabv3+: Deep learning for semantic image segmentation," *arXiv preprint arXiv:1802.02611*, 2017.
[31] Z. Zhou, M. M. Rahman Siddiquee, N. Tajbakhsh, and J. Liang, "Unet++: A nested u-net architecture for medical image segmentation," in *International workshop on deep learning in medical image analysis*, 2018: Springer, pp. 3-11.
[32] O. Oktay *et al.*, "Attention u-net: Learning where to look for the pancreas," *Medical Image Analysis*, vol. 53, pp. 129–139, 2018.
[33] O. Ronneberger, P. Fischer, and T. Brox, "U-net: Convolutional networks for biomedical image segmentation," in *International Conference on Medical image Computing and Computer-assisted Intervention*, 2015: Springer, pp. 234-241.
[34] L. Breiman, "Random forests," *Machine Learning*, vol. 45, no. 1, pp. 5-32, 2001/10/01 2001. 10.1023/A:1010933404324
[35] A. Liaw and M. Wiener, "Random forests for classification and regression," *R News*, vol. 2, no. 3, pp. 18–22, 2002.
[36] A. Géron, "A gentle introduction to random forests," Toward Data Science, 2017. https://towardsdatascience.com
[37] G. Biau, "Random forests: An overview," *Statistical Interface*, vol. 2, no. 3, pp. 359–368, 2012.